Chemical Engineering Journal 195–196 (2012) 40–48

Contents lists available at SciVerse ScienceDirect

Chemical Engineering Journal

journal homepage: www.elsevier.com/locate/cej

Efficient adsorptive removal of phenol by a diethylenetriamine-modified hypercrosslinked styrene–divinylbenzene (PS) resin from aqueous solution

Jianhan Huang [a,b,*], Hongwei Zha [a], Xiaoying Jin [a], Shuguang Deng [c]

[a] School of Chemistry and Chemical Engineering, Central South University, Changsha 410083, China
[b] Key Laboratory of Resources Chemistry of Nonferrous Metals, Ministry of Education, Changsha 410083, China
[c] Chemical Engineering Department, New Mexico State University, Las Cruces, NM 88003, USA

HIGHLIGHTS

- A diethylenetriamine-modified hypercrosslinked PS resin was synthesized.
- More excellent equilibria, kinetics and dynamics of HJ-M05 than the others.
- Equilibria, kinetics and dynamics characterized by several models.
- Surface energetic heterogeneity characterized by the Do's model.
- Good agreement between dynamic and equilibrium capacities.

ARTICLE INFO

Article history:
Received 18 March 2012
Received in revised form 26 April 2012
Accepted 27 April 2012
Available online 7 May 2012

Keywords:
Adsorption
Phenol
Polymeric adsorbent
XAD-4
XAD-7

ABSTRACT

Phenol is a typical organic pollutant in industrial wastewater and efficient adsorptive removal of phenol from aqueous solution has attracted many attentions in recent years. In the present study, a diethylenetriamine-modified hypercrosslinked styrene–divinylbenzene (PS) resin, HJ-M05, was synthesized, characterized and evaluated for adsorptive removal of phenol from aqueous solution, and two typical commercial polymeric adsorbents, Amberlite XAD-4 and XAD-7, were employed as references. The equilibrium capacity on HJ-M05 was much larger than those on XAD-4, XAD-7 and the precursor, HJ-55. The degree of the surface energetic heterogeneity of HJ-M05 was proven to be higher than XAD-4 and XAD-7 while the adsorbate–adsorbate interaction of the adsorbed phenol molecules on HJ-M05 was much less than that on XAD-4 and XAD-7. The kinetic data on HJ-M05 could be well plotted by the micropore diffusion model while those on XAD-4 and XAD-7 could not be fitted by this model. Thomas and Yoon models were more suitable for describing the dynamic data than the Clark model and the dynamic capacities on HJ-M05, HJ-55, XAD-4 and XAD-7 were calculated to be 201.7, 178.1, 107.5 and 74.80 mg/g dry resin, respectively. 15.0 BV (1 BV = 10 ml) 1% of sodium hydroxide could regenerate the HJ-M05 resin column completely and the dynamic desorbed amount was almost equal to the dynamic adsorption amount.

1. Introduction

Phenol (C_6H_5OH) is a typical organic pollutant in industrial wastewater [1,2]. Because of its importance in industry, many methods are developed for production of phenol while it is currently produced by partial oxidation of isopropylbenzene via the Hock rearrangement. Phenol is a versatile raw material to synthesize a large number of chemicals such as bisphenol-A, salicylic acid and cyclohexanone, which are typical precursors to produce plastics, polycarbonates, epoxide resins and phenolic resins. Phenol can also be applied to synthesize drugs, herbicides and pharmaceuticals [3–5]. However, due to its hydrophobic effect and it can be formed as phenoxyl radicals in the human's body, phenol is considered as a highly toxic organic pollutant to human being. Phenol and its vapors are corrosive to the eyes, skin and respiratory tract. It may also cause harmful effects on lung, liver, kidneys and even central nervous system and heart. Consequently, efficient removal and recycling of phenol from aqueous solution has received many attentions in recent years.

Adsorption of organic pollutants from aqueous solution by polymeric adsorbents has proven to be an economical and effective method due to the relatively good mechanical strength, large capacity, high selectivity and diverse chemical structure of the synthesized polymeric adsorbents [6–9]. Moreover, the polymeric

* Corresponding author at: School of Chemistry and Chemical Engineering, Central South University, Changsha 410083, China. Tel./fax: +86 731 88879616.
E-mail addresses: jianhanhuang@csu.edu.cn (J. Huang), sdeng@nmsu.edu (S. Deng).

1385-8947/$ - see front matter © 2012 Elsevier B.V. All rights reserved.
http://dx.doi.org/10.1016/j.cej.2012.04.098

adsorbents can be easily regenerated by some typical organic reagents and the organic pollutants adsorbed on the polymeric adsorbents can be recycled successfully, and hence the polymeric adsorbents are receiving increasing attentions and they are considered as the powerfully potential alternative for the extensively used activated carbon [10–12]. Amberlite XAD-4, developed by Rohm & Haas Company, is one of the best commercial polymeric adsorbents of the second generation styrene–divinylbenzene (PS) copolymers for removing organic pollutants from aqueous solution [13,14], and many experimental studies have demonstrated that XAD-4 is very effective for adsorption of non-polar or weakly polar aromatic compounds such as toluene, phenol and β-naphthol from aqueous solution although a careful pre-treatment process is required before using [15–17]. Amberlite XAD-7 is another efficient polymeric adsorbent for adsorption of peptides and proteins due to its acrylic ester structure [18,19]. Moreover, the relatively large pores of XAD-7 make it an ideal candidate for adsorption of large polar molecules like dyes [20]. In recent years, the hypercrosslinked PS resins are recognized as a kind of super polymeric adsorbents for adsorptive removal of aromatic compounds from aqueous solution due to their unique pore structure [21–23]. In particular, surface chemical modification of the hypercrosslinked PS resins by introduction of some specific functional groups like amino groups on the surface of the hypercrosslinked PS resins makes them even more effective [24–26].

In general, equilibria, kinetics and dynamics are three essential and important aspects for evaluating the efficacy of an adsorbent [27]. Adsorption equilibria can be applied to preliminarily screen the adsorbents and it provides a measure of the adsorption efficacy for removal of a specific adsorbate. In addition, some typical thermodynamic parameters such as adsorption enthalpy ΔH (kJ/mol), Gibbs free energy ΔG (kJ/mol) and entropy ΔS (kJ/(mol K)) can be calculated by analyzing the adsorption equilibria (the equilibrium isotherms at different temperatures) [28]. Adsorption kinetics are of great significance for assessing the kinetic performance of a given adsorbent, which allow us to gain insight into the underlying adsorption mechanisms. From a practical point of view, the involved kinetic behaviors are the primary industrial focus of attention [29]. Adsorption dynamics play a dominant role in appraising of the efficacy of an adsorbent during a continuous column operation. The dynamic adsorption does not necessarily run under equilibrium conditions, and hence the hydrodynamics and the mass transfer of the adsorbates in the column are two peculiar aspects to be considered in addition to a particular length-to-diameter ratio of the column [7].

In the current study, we firstly prepared a diethylenetriamine-modified hypercrosslinked styrene–divinylbenzene (PS) resin, HJ-M05, by a self Friedel–Crafts reaction of chloromethylated PS and a nucleophilic substitution reaction of the obtained precursor, HJ-55, with diethylenetriamine. After characterization of the adsorbent, we assessed the adsorptive removal ability of HJ-M05 from aqueous solution. Phenol, as the typical organic pollutant, was selected as the adsorbate, and Amberlite XAD-4 and XAD-7 were employed as references. Based on the different adsorption behaviors, the potential application of HJ-M05 for satisfactory adsorptive removal of phenol from an aqueous solution was exploited.

2. Materials and methods

2.1. Materials

Chloromethylated PS was purchased from Langfang Chemical Co. Ltd. (Hebei province, China), its cross-linking degree was 6%, its chlorine content was measured to be 17.3%, its BET surface area and pore volume were determined to be 28 m^2/g and 0.0036 cm^3/g, respectively. Phenol applied as the adsorbate in this study was used after distillation, 1, 2-dichloroethane used as the solvent was anhydrate by mesoporous molecular sieve before using, diethylenetriamine and iron (III) chloride were analytical reagents and used without further purification.

2.2. Synthesis of the adsorbent

Twenty-five gram of chloromethylated PS was firstly swollen in 120 ml of 1, 2-dichloroethane overnight and 5.0 g of iron (III) chloride was then added into the reaction mixture with the temperature at 323 K. After the added iron (III) chloride was completely dissolved, the reaction mixture was refluxed for 5 h and the obtained hypercrosslinked PS resin named HJ-55 was thereafter mixed with 60 ml of diethylenetriamine and the reaction mixture was kept at 413 K for 20 h, and hence the diethylenetriamine-modified hypercrosslinked PS resin, HJ-M05 (the water retention capacity of the HJ-M05 was measured to be 57.4%), were prepared.

2.3. Adsorption equilibria

For the equilibra of phenol adsorption on the adsorbents, about 0.1000 g of the adsorbents was accurately weighed and added into 50 ml of phenol aqueous solution with different initial concentrations, C_0 (mg/L), in a series of 100 ml of conical flasks with stoppers. Dry HJ-55 and HJ-M05 were used directly in the experiments due to their high hydrophilicity to water while wet XAD-4 and XAD-7 were used after a careful pre-treatment. At a desired temperature, the flasks were then shaken in a water-bathing thermostatic oscillator until the adsorption equilibrium was reached, the equilibrium concentration of phenol aqueous solution, C_e (mg/L), was determined and the equilibrium capacity of phenol on the adsorbent, q_e (mg/g), was calculated as:

$$q_e = (C_0 - C_e)V/W \quad (1)$$

where V was the volume of the aqueous solution (L) and W was the weight of the adsorbent (g).

2.4. Adsorption kinetics

For the kinetics of phenol adsorption on the adsorbents, about 1.0000 g of the adsorbents was mixed with 250 ml of phenol aqueous solution at an initial concentration of 518.7 mg/L in a 500 ml of conical flask with a stopper. The flask was then continuously shaken in a water-bathing thermostatic oscillator at a preset temperature (303, 308 or 313 K) until the adsorption equilibrium was reached. During the shaking process, 0.5 ml of phenol aqueous solution was withdrawn at a 10-min interval in the first 1 h and a 30-min interval in the subsequent hour, and the concentration of phenol aqueous solution at contact time t, C_t (mg/L), was determined and the adsorption capacity at contact time t, q_t (mg/g), was calculated based on the equation as follows:

$$q_t = (C_0 - C_t)V/W \quad (2)$$

2.5. Adsorption and desorption dynamics

For the adsorption and desorption dynamics of phenol on the adsorbents, the adsorbents were firstly immersed in de-ionized water overnight at room temperature and then 10 ml of wet adsorbents (weight of the dry adsorbents was measured to be 3.51, 3.24, 2.87 and 2.69 g for HJ-M05, HJ-55, XAD-4 and XAD-7) were packed in a glass column (inner diameter: 16 mm) densely with no bubbles between the solid particles in the column. The phenol aqueous solution at an initial concentration of 1000.0 mg/L was passed through the glass column at a flow rate of 12.0 BV/h (1 BV = 10 ml)

and the concentration of phenol aqueous solution of the effluent from the column, C (mg/L), was continuously recorded until that was almost equal to the initial one. After this process, the adsorbents in the glass column were roughly rinsed by 10 ml of de-ionized water and 1% of sodium hydroxide aqueous solution was applied as the solvent to the desorption process. 200 ml of sodium hydroxide aqueous solution was passed through the resin column at a flow rate of 6.8 BV/h and the concentration of phenol was determined until that was close to zero.

2.6. Analysis

The chorine content of the adsorbents was measured by the Volhard method [30] and the weak basic exchange capacity of the adsorbents was determined by another established method in ref [31]. The pore structure parameters of the samples were determined from the N_2 adsorption–desorption isotherms 77 K using a Micromeritics Tristar 3000 surface area and porosity analyzer. The total surface area and pore volume of the adsorbents were calculated according to Brunauer–Emmett–Teller (BET) model while the micropore surface area and micropore volume were calculated by the Barrett, Joyner and Halenda (BJH) method, the pore diameter distribution of the adsorbents was determined by applying BJH method to the N_2 desorption data. The Fourier transform infrared spectroscopy (FT-IR) of the adsorbents was collected by KBr disks on a Nicolet 510P Fourier transformed infrared instrument. The morphology, composition and size of the adsorbents were carried out by scanning electron microscopy (SEM) equipped with energy-dispersive X-ray spectroscopy (EDS). The concentration of phenol in aqueous solution was analyzed by UV analysis performed on a Perkin–Elmer Lambda 17 UV spectrophotometer with the wavelength at 269.9 nm.

3. Results and discussion

3.1. Characteristics of the adsorbent

After the Friedel–Crafts reaction, the chlorine content of the sample decreased from 17.3% (the chloromethylated PS) to 3.15% (HJ-55) and the vibration related to the C–Cl stretching of CH_2Cl groups (at 1265 cm^{-1}) was much weakened in the FT-IR spectrum (see Fig. 1a), implying that the chlorine of the chloromethylated PS was consumed in the Friedel–Crafts reaction. After the nucleophilic substitution reaction of HJ-55 with diethylenetriamine, the chlorine content further reduced to 0.51% and 1.804 mmol/g of weak basic exchange capacity was measured for HJ-M05, meaning that the residual chlorine on the surface of HJ-55 was nucleophilically substituted by the amino groups (–NH–/–NH_2) of diethylenetriamine and this deduction can be confirmed by the vibrations at 3426 cm^{-1} (N–H stretching), 1501 cm^{-1} (N–H deformation) and 1109 cm^{-1} (C–N stretching) in the FT-IR spectrum for HJ-M05.

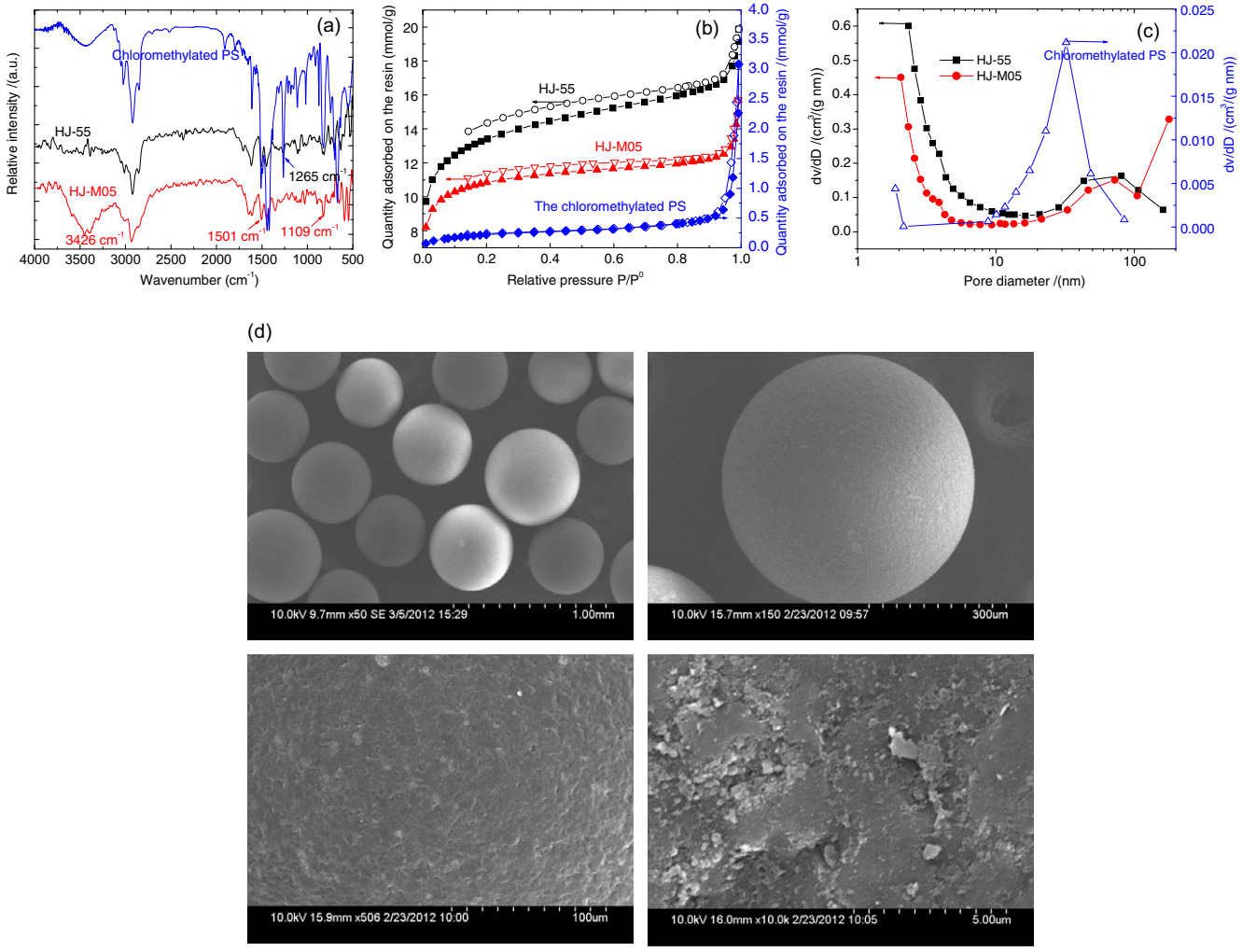

Fig. 1. Characterization of the hypercrosslinked styrene–divinylbenzene resin, HJ-M05, in comparison with the chloromethylated PS and the precursor, HJ-55. (a) FT-IR; (b) N_2 adsorption–desorption isotherms; (c) pore diameter distribution; (d) SEM.

Fig. 1b indicated that the Friedel–Crafts reaction caused an greatly increased N_2 adsorption amount from about 0.5 mmol/g (the chloromethylated PS) to about 15.0 mmol/g (HJ-55), suggesting that there should be a rapid increase of the BET surface area and pore volume while a sharp decrease of the pore size for the obtained sample (BET surface area and pore volume of HJ-55 were measured to be 941.7 m^2/g and 0.6137 cm^3/g while those of the chloromethylated PS were 28 m^2/g and 0.0036 cm^3/g, respectively). Moreover, decrease of the pore size produces a large number of micropores for HJ-55 (see Fig. 1c) and the *t*-plot micropore surface area and *t*-plot micropore volume are determined to be 514.2 m^2/g and 0.2768 cm^3/g, respectively.

After the nucleophilic substitution reaction of HJ-55 with diethylenetriamine, the N_2 adsorption amount decreased from about 15.0 mmol/g (HJ-55) to about 11.0 mmol/g (HJ-M05) due to the increased polarity (uploading of –NH–/–NH_2 on the surface of HJ-M05), the decreased BET surface area and pore volume (746.4 m^2/g and 0.4487 cm^3/g). In addition, it is interesting to observe that the pore size of the adsorbent in the micropore region tends to further lessen after the nucleophilic substitution reaction. The scanning electron microscopy (SEM) images of HJ-M05 in Fig. 1d indicate that HJ-M05 is a spherical solid particle with the particle size of about 0.55 mm and its surface is very rough with many fissures.

3.2. Adsorption comparison

For the Friedel–Crafts reaction of the chloromethylated PS, it is reported that the residual chlorine content of the product strictly relies on the Friedel–Crafts reaction time and the longer time reaction results in lower residual chlorine content of the product [32]. We believe that the residual chlorine content of the product should determine its pore structure and a hypercrosslinked resin with lower residual chlorine content should have a higher BET surface area and pore volume. In addition, as the residual chlorine can be further nucleophilically substituted by nucleophilic reagents and some polar groups are uploaded on the surface of the hypercrosslinked resin, the hypercrosslinked resin with higher residual chlorine content will upload more polar groups, inducing a higher polarity for the chemical modified hypercrosslinked resin. Therefore, it is possible for us to adjust the pore structure as well as the polarity of the hypercrosslinked resin by simply adjusting the Friedel–Crafts reaction time of the chloromethylated PS, and which determines their adsorption selectivity.

In this study, we synthesized some other kind of diethylenetriamine-modified hypercrosslinked PS resins labeled HJ-M01, HJ-M03 and HJ-M09 by adjusting the Friedel–Crafts reaction time as 1 h, 3 h and 9 h, respectively. As compared the equilibrium capacity of phenol adsorption on these series of adsorbents at the same initial concentration of phenol and the same temperature (see Fig. S1a), it is observed that HJ-M05 possesses the largest equilibrium capacity among these four adsorbents. HJ-M05 should not have the highest BET surface area and pore volume due to its shorter Friedel–Crafts reaction time than that of HJ-M09, and it also should not have the highest amount of the functional groups (–NH–/NH_2) on the surface by the reason of its lower residual chlorine content in contrast with HJ-M01 and HJ-M03. However, the combinations of the appropriate pore structure and the appropriate uploading amount of the functional groups help to bring a better phenol adsorption on HJ-M05. The present results imply that the appropriate pore structure and the appropriate surface polarity of an adsorbent are two primary criterions to assess the efficacy of an adsorbent for adsorption of a specific adsorbate.

Fig. S1b compares the isotherms of phenol adsorption on HJ-55 and HJ-M05, the equilibrium capacity of phenol adsorption on HJ-M05 is obviously larger than that on HJ-55 at the same equilibrium concentration and temperature. Although there is an obvious decrease of the BET surface area and pore volume after the nucleophilic substitution reaction (the reduction magnitude of the BET surface area and pore volume were 195.3 m^2/g and 0.1650 cm^3/g, respectively), the uploaded –NH–/NH_2 on the surface of HJ-M05 might make the adsorption enhanced due to the polarity matching and the possible hydrogen bonding between the –NH–/NH_2 of HJ-M05 and the phenolic –OH of phenol [33]. Of course, the micropore filling may also play a role due to the smaller pore size of HJ-M05 in the micropore region contrasted with HJ-55 [34].

3.3. Adsorption isotherms

Fig. 2a describes the isotherms of phenol adsorption on HJ-M05 from aqueous solution with the temperature at 303, 308 and 313 K,

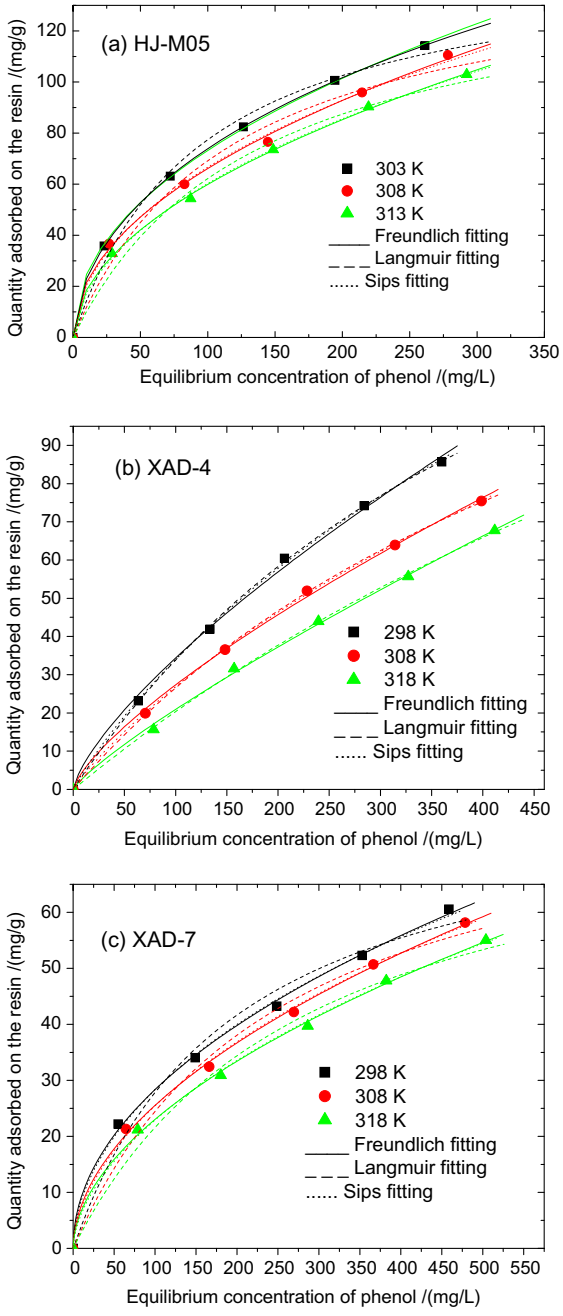

Fig. 2. Equilibrium isotherms for phenol adsorption on (a) HJ-M05; (b) XAD-4; (c) XAD-7 from aqueous solution.

respectively. As a reference, the Amberlite XAD-4 and XAD-7 are employed as two typical commercial polymeric adsorbents and their isotherms towards phenol are also shown in Fig. 2b and c. The adsorption is weakened with increasing of the temperature for the three adsorbents. At an equilibrium concentration of 200 mg/L and the temperature of 308 K, the equilibrium capacities of phenol on HJ-M05, XAD-4 and XAD-7are measured to be 92.43, 46.04 and 36.49 mg/g, respectively, following an order of $q_{e(\text{HJ-M05})} > q_{e(\text{XAD-4})} > q_{e(\text{XAD-7})}$, which suggested that HJ-M05 is superior to the commercial polymeric adsorbent for the phenol adsorption.

XAD-4 is deemed as one of the best mesoporous (average pore diameter is about 5.8 nm) polymeric adsorbents of the second generation styrene–divinylbenzene copolymers for adsorptive removal of non-polar or weakly polar aromatic compounds from aqueous wastes, groundwater and vapor streams. However, XAD-4 is proven to be inferior to HJ-M05 in this study. The BET surface area and pore volume of XAD-4 (750 m^2/g and 0.98 cm^3/g) is higher than those of HJ-M05, while the abundant micropores will enhance the phenol adsorption on HJ-M05 due to micropore filling mechanism [34,35]. In particular, the uploaded –NH–/NH_2 on the surface of HJ-M05 can be acted as hydrogen bonding acceptors and form hydrogen bonding with the phenolic –OH of phenol, and the specific polarity interaction (hydrogen bonding) enhances the adsorption. XAD-7 is an efficient polymeric adsorbent for adsorption of polar compounds such as peptides, proteins and dyes due to its acrylic ester structure and relatively large pores (average pore diameter is about 7.4 nm). However, the relatively lower BET surface area (450 m^2/g) and larger pore diameter of XAD-7 make it a relatively poor adsorbent for adsorption of phenol in the present study. In addition, hydrogen bonding should be the main driving force for the adsorption of phenol on XAD-7 from aqueous solution. Before phenol can be adsorbed on XAD-7, the other two hydrogen bonding between XAD-7 and water as well as that between phenol and water should be broken, which reduces the phenol adsorption capacity on XAD-7.

Langmuir, Freundlich and Sips models are three typical adsorption models to describe the adsorption process [36–38]. They can be described as:

Langmuir equation:

$$q_e = \frac{K_L C_e q_m}{1 + K_L C_e} \tag{3}$$

Freundlich equation:

$$q_e = K_F C_e^{1/n} \tag{4}$$

Sips equation:

$$q_e = \frac{q_m K C_e^{1/n}}{1 + K C_e^{1/n}} \tag{5}$$

where q_m is the maximum adsorption capacity (mg/g), K_L is the Langmuir constant (L/mg), K_F [(mg/g)(L/mg)$^{1/n}$] and n are the Freundlich constants and K is the Sips constant.

The three isotherm models were adopted to describe the equilibrium data by a non-linear fitting and the sum of squares due to error (SSE) was used to assess the correlation. As can be observed from Tables S1–S3, the Langmuir and Sips equations are more suitable for the phenol adsorption on XAD-4 than the Freundlich equation while the Freundlich and Sips equations are more appropriate for characterizing the phenol adsorption on HJ-M05 and XAD-7.

According to Clausius–Clapeyron equation [39,40], the isosteric adsorption enthalpies (ΔH, kJ/mol) for the phenol adsorption on HJ-M05, XAD-4 and XAD-7 were calculated at a given fractional loading (θ, $\theta = q_e/q_m$), and the results were displayed in Fig. 3. It is found that the ΔH on the three adsorbents follows an order as

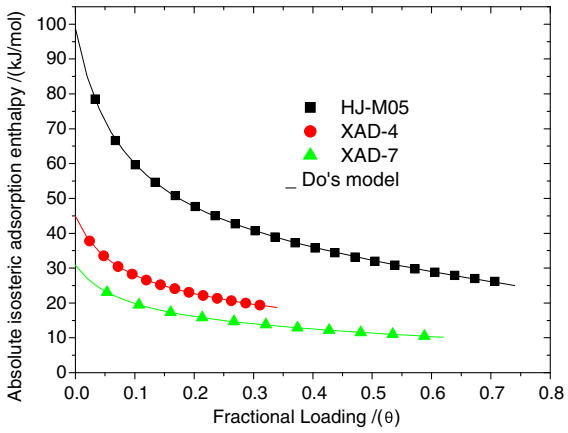

Fig. 3. Plotting of the isosteric adsorption enthalpies versus the factional loading for the phenol adsorption on HJ-M05, XAD-4 and XAD-7.

$\Delta H_{(\text{HJ-M05})} > \Delta H_{(\text{XAD-4})} > \Delta H_{(\text{XAD-7})}$ at the same fractional loading, which suggests that the interaction between HJ-M05 and phenol is the greatest while that between XAD-7 and phenol is the least. Additionally, the ΔH decreases greatly with increasing of the fractional loading, indicating a surface energetic heterogeneity of the three adsorption systems. At a lower fractional loading, phenol molecules are preferably adsorbed on the most exposed sites of the adsorbent with a higher energy and hence the ΔH is relatively higher. As these sites are gradually occupied by phenol molecules and saturated, the adsorbate–adsorbent interaction is mainly dispersed and the subsequent phenol molecules have to be adsorbed on the sites with a relatively lower energy and which induces the ΔH less.

To expound the surface energetic heterogeneity of HJ-M05, XAD-4 and XAD-7, Do's model is employed in this study [41]. Do's model assumes that the degree of the surface energetic heterogeneity of a solid is reflected by the variation of the isosteric adsorption enthalpy (ΔH) as a function of the fractional loading of the adsorbate (θ) as:

$$\Delta H = \Delta H_0\{1 - \alpha\beta\theta/[1 + (\beta - 1)\theta]\} + \mu\theta \tag{6}$$

where ΔH_0 is the isosteric adsorption enthalpy at $\theta = 0$, α is the variation ratio of the isoteric adsorption enthalpy with θ from 0 to 1 and it reflects the extent of the surface energetic heterogeneity of the adsorbent. β is the pattern parameter of the adsorbent, and a higher β suggests a faster decreasing speed for the isosteric adsorption enthalpy at the initial adsorption stage while a slower one near the monolayer coverage loading. μ is the adsorbed adsorbates–adsorbates interaction parameter on the adsorbent.

We used a non-linear regression method to correlate the data (ΔH versus θ) and the fitting results are revealed in Fig. 3, the corresponding constants ΔH_0, α, β and μ as well as SSE are summarized in Table 1. The SSE in Table 1 indicates that the fitted results are reliable, which implies that Do's model can describe the surface energetic heterogeneity of the adsorbents effectively. ΔH_0 for the phenol adsorption on HJ-M05 is particularly negative, which is about twice and three times greater than those on XAD-4 and

Table 1
Fitted constants for the surface energetic heterogeneity of HJ-M05, XAD-4 and XAD-7 according to Do's model.

	H_0 (kJ/mol)	α	β	μ	SSE
HJ-M05	−98.78	0.6158	13.89	−19.50	0.6008
XAD-4	−44.89	0.5588	15.15	−11.70	0.007015
XAD-7	−30.84	0.5706	13.02	−6.245	0.009069

XAD-7. This result suggested a rather different adsorption mechanism for the phenol adsorption on HJ-M05. π–π stacking is proven to be main interaction between XAD-4 and phenol and hydrogen bonding is the main driving force the phenol adsorption on XAD-7 [14,42]. There should be multiple adsorbent–adsorbate interactions between HJ-M05 and phenol and these interactions include π–π stacking and hydrogen bonding, but even more important, micropore filling is the most predominant mechanism [34,35]. α of HJ-M05, XAD-4 and XAD-7 are predicted to be 0.6158, 0.5588 and 0.5706, implying that the extent of surface energetic heterogeneity of HJ-M05 is the greatest while XAD-4 is the most homogeneous adsorbent among the three adsorbents. On the contrary, μ of HJ-M05 is the most negative, suggesting that the adsorbed adsorbate–adsorbate interaction on the surface of HJ-M05 is not worthy mentioning in comparison with the adsorbate-adsorbent interaction and it confirms that HJ-M05 is an efficient polymeric adsorbents for adsorption of phenol from aqueous solution.

3.4. Adsorption kinetics

Fig. 4 displays the kinetic curves for phenol adsorption on HJ-M05 with the initial concentration at 518.8 mg/L and the temperature at 303, 308 and 313 K, respectively. As a reference, the kinetic curves of phenol adsorption on XAD-4 and XAD-7 are also shown in Fig. 4. The adsorption capacity of phenol on HJ-M05 is quite larger than those on XAD-4 and XAD-7 at the same initial concentration and temperature, which is coincident with the equilibrium results mentioned above. In addition, the required time from the beginning to the equilibrium for the phenol adsorption on the three adsorbents is quite different, XAD-4 and XAD-7 only require less than 60 min to reach equilibrium while at least 200 min is required for the adsorption on HJ-M05 and the adsorption at a higher temperature needs shorter time due to the faster diffusion speed.

Lagergren's rate equation (pseudo-first-order rate equation) and pseudo-second-order equation are two typical kinetic models to describe the kinetic data [43,44]. They can be described as:

$$\text{Pseudo-first-order rate equation}: \ \ln(1-F) = -k_1 \times t \tag{7}$$

$$\text{Pseudo-second-order rate equation}: t/q_t = 1/(k_2 \times q_e^2) + t/q_e \tag{8}$$

here k_1 is the pseudo-first-order rate constant (min^{-1}), F is the fractional attainment of the equilibrium as $F = q_t/q_e$ and k_2 is the pseudo-second-order rate constant (g/(mg min)).

Table S4 summarizes the corresponding parameters by fitting the experimental data to the pseudo-first-order and pseudo-second-order rate equations via a non-linear fitting method. It is interesting to see that both of pseudo-first-order and pseudo-second-order rate equations are suitable for the phenol adsorption on XAD-4 and XAD-7, while the adsorption on HJ-M05 can only be fitted by the pseudo-second-order rate equation. In addition, the fitted k_2 of XAD-7 and XAD-4 is obviously greater than those of HJ-M05, and a greater k_2 is presented at a higher temperature for the phenol adsorption on HJ-M05, which is accordant with the above observations that XAD-4 and XAD-7 require shorter time to reach equilibrium than HJ-M05 and the required time is shorter at a higher temperature for the phenol adsorption on HJ-M05.

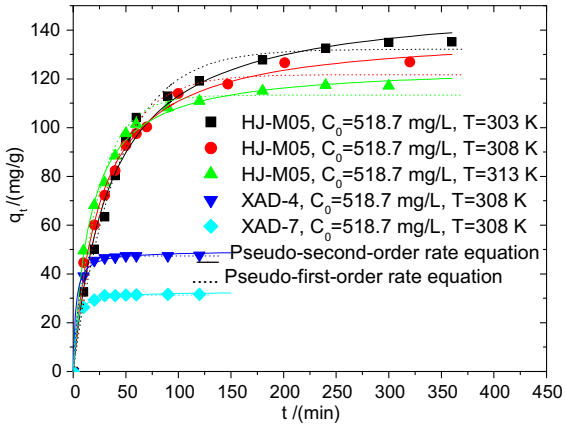

Fig. 4. Kinetic adsorption curves of phenol on HJ-M05, XAD-4 and XAD-7 from aqueous solution.

As mentioned in the previous section, a large number of micropores were existent and the microporous region was the concentrating distribution for the pore of HJ-M05, and hence a micropore diffusion model was applied in the present study to further analyze the kinetic data, the diffusion time constant as well as the diffusion activation energy (E_a, kJ/mol) could also be gained [45]. For the fractional adsorption uptake (q_t/q_e) less than 85%, the adsorption kinetics in a microporous adsorbent can be demonstrated as:

$$\frac{q_t}{q_e} = \frac{6}{\sqrt{\pi}}\sqrt{\frac{D_c t}{r_c^2}} - \frac{3D_c t}{r_c^2} \tag{9}$$

where D_c is the micropore diffusion parameter (cm^2/s) and r_c is the particle diameter of the adsorbent (cm).

The kinetic curves in Fig. 4 were firstly converted to the plotting of q_t/q_e versus t and then the obtained curves were fitted by the micropore diffusion model through a non-linear regression (see Fig. S2). It is clear that the micropore diffusion model can describe the curves of plotting of q_t/q_e versus t for the phenol adsorption on HJ-M05 while the kinetic data for the phenol adsorption on XAD-4 and XAD-7 cannot be fitted by this micropore diffusion model, which in turn implies that HJ-M05 is a microporous adsorbent but XAD-4 and XAD-7 are not. The diffusion time constants (D_c/r_c^2) obtained from the non-linear regression were listed in Table 2, which can be applied to calculate the diffusion activation energy of 41.22 kJ/mol by plotting of D_c/r_c^2 versus $1/T$ (see Fig. S3).

3.5. Dynamic adsorption and desorption

Fig. 5 presents the dynamic curves for phenol adsorption on HJ-M05 from aqueous solution with an initial concentration of phenol at 1000.0 mg/L and a flow rate at 120 ml/h. As a comparison, the dynamic curves for phenol adsorption on HJ-55, XAD-4 and XAD-7 are also shown in Fig. 5. The breakthrough point (at $C/C_0 = 0.05$) for phenol adsorption on HJ-M05, HJ-55, XAD-4 and XAD-7 is measured to be 43.0, 38.2, 20.1 and 11.8 BV respectively, which further confirms that HJ-M05 is the most efficient adsorbent for adsorptive removal of phenol from aqueous solution among these four adsorbents. According to a numerical integration method shown in Eq. (10), the dynamic adsorption amounts of phenol adsorption on HJ-M05, HJ-55, XAD-4 and XAD-7 are calculated to be 708.1, 576.9, 308.5, 201.2 mg, respectively. Taking into consideration of the weight of the adsorbents, the dynamic adsorption capacities of phenol on these four adsorbents can be calculated to be 201.7, 178.1, 107.5 and 74.80 mg/g dry resin, respectively. These data show a deviation about 10% the extrapolated values

Table 2
Correlated parameters of the kinetic data for the phenol adsorption on HJ-M05 from aqueous solution according to the micropore diffusion model.

T (K)	D_c/r_c^2 (min^{-1})	SSE
303	1.098×10^{-3}	0.02938
308	1.358×10^{-3}	0.003098
313	1.853×10^{-3}	0.009550

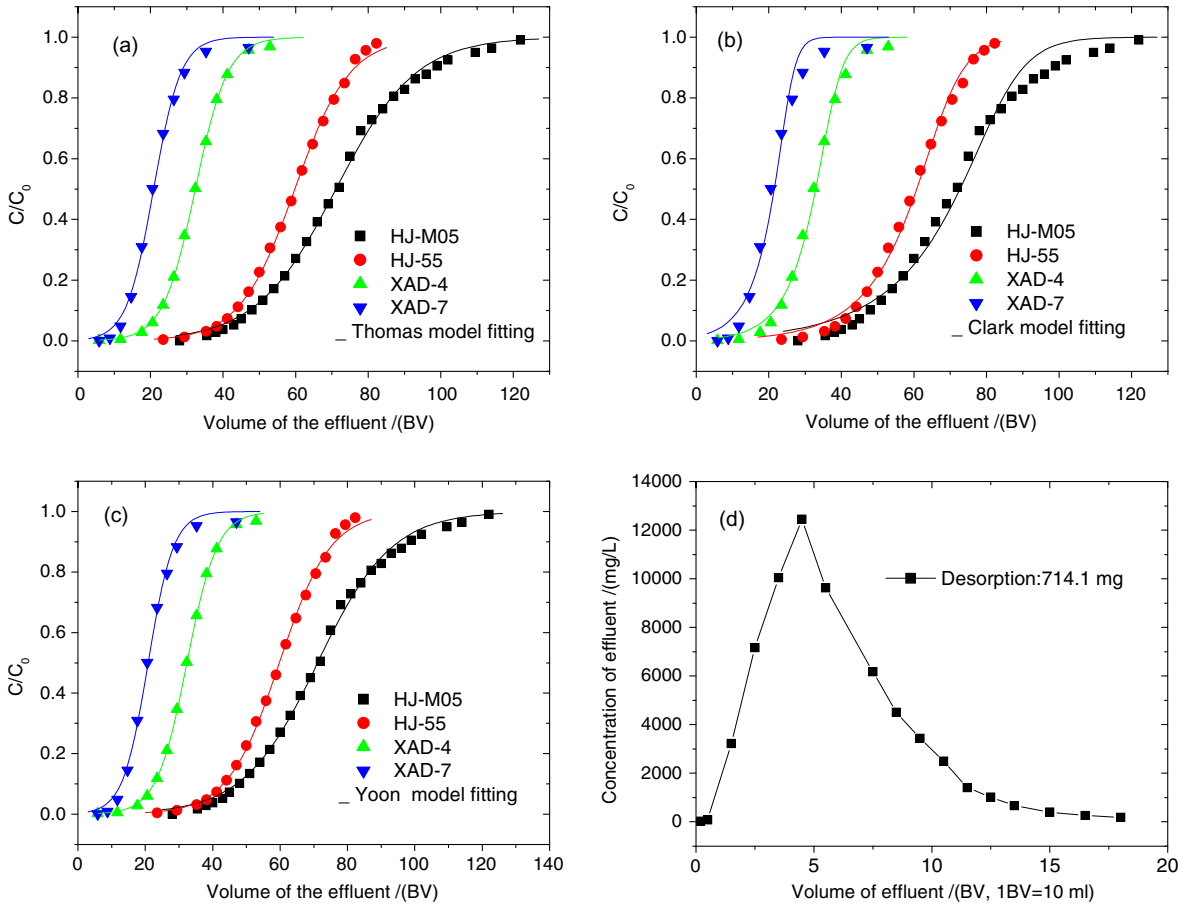

Fig. 5. Dynamic adsorption–desorption of phenol on HJ-M05, XAD-4 and XAD-7 from aqueous solution. (a) Fitted by Thomas model; (b) fitted by Clack model; (c) fitted by Yoon model; (d) desorption curve of phenol from HJ-M05.

from the Freundlich models (216.3, 201.7, 185.8 and 87.43 mg/g, respectively), which suggest that the dynamic experimental results match well with the batch adsorption equilibrium data.

$$q_{dynamic}\left(\frac{\text{mg}}{\text{g}}\right) = \left\{\int_0^{\text{BV}_{\max}} \left(1-\frac{C_V}{C_0}\right)\text{dBV}\right\} * C_0\left(\frac{\text{mg}}{\text{L}}\right) * \frac{10\ (\text{ml})}{3\ (\text{g})} * \frac{1\ (\text{L})}{1000\ (\text{mL})} \quad (10)$$

Thomas, Clark and Yoon models are three typical models for characterizing the dynamic properties of an adsorbent [46–48]. They can be arranged as:

Thomas model:

$$\frac{C}{C_0} = \frac{1}{1+\exp[k_T(q_0 m_C - C_0 V_{eff})/Q]} \quad (11)$$

Clark model:

$$\frac{C}{C_0} = \left(\frac{1}{1+Ae^{-rV_{eff}/Q}}\right)^{1/n-1} \quad (12)$$

Yoon model:

$$\frac{C}{C_0} = \frac{\exp(k_{YN}V_{eff}/Q - K_{YN}t_{0.5})}{1+\exp(k_{YN}V_{eff}/Q - K_{YN}t_{0.5})} \quad (13)$$

where C and C_0 are the concentration of the adsorbate from the effluent and that at the initial state (mg/ml), k_T is the Thomas rate constant [ml/(min mg)], q_0 is the maximum adsorption capacity (mg/g), m_C is the weight of the adsorbent in the column (g), V_{eff} is the throughput volume (ml) and Q is the volumetric flow rate (ml/min). n is the Freundlich constant and A and r are the Clark constants related to the breakthrough point. k_{YN} is the Yoon rate constant (min^{-1}) and $t_{0.5}$ is the required time for the 50% breakthrough concentration from a fixed bed of an adsorbent.

The three models are used to fit the dynamic curves by a nonlinear regression and the fitting curves are presented in Fig. 5a, b and c, respectively. Table S5 summarizes the corresponding parameters. Thomas and Yoon models are shown to be more suitable for fitting the dynamic data than the Clark model due to a lesser SSE. q_0 for the phenol adsorption on HJ-M05, HJ-55, XAD-4 and XAD-7 calculated by the Thomas model are determined to be 202.6, 184.5, 112.7 and 77.63 mg/g, respectively, which are very close to the corresponding experimental capacities (201.7, 178.1, 107.5 and 74.80 mg/g) discussed in the previous section. In addition, k_{YN} predicted by the Yoon model is identical to corresponding k_T by the Thomas model and the $t_{0.5}$ is calculated to be 355.7, 298.9, 161.5 and 104.4 min for HJ-M05, HJ-55, XAD-4 and XAD-7, respectively, these data are very close to the experimental data (360.2, 300.8, 159.5 and 104.6 min, respectively), which further states that the Thomas and Yoon models characterize the dynamic data excellently.

After the dynamic adsorption experiment, the HJ-M05 resin column was roughly purged with 10 ml of de-ionized water and then 200 ml 1% of sodium hydroxide aqueous solution was passed through the resin column to desorb the phenol molecules on the resin. As can be seen from Fig. 5d, only 15.0 bed volumes of 1% of sodium hydroxide solution were needed to completely regenerate the resin column and the dynamic amount of phenol desorbed from the resin column was determined to be 714.1 mg, which is

excellently coincident with the dynamic adsorption amounts of phenol adsorption on HJ-M05.

4. Conclusions

We synthesized a diethylenetriamine-modified hypercross-linked PS resin, HJ-M05, by a self Friedel–Crafts reaction of chloromethylated PS and a nucleophilic substitution reaction of the obtained precursor with diethylenetriamine. The chemical and pore structure of the adsorbent was characterized by the chemical analysis (chlorine content, weak basic exchange capacity), FT-IR, N_2 adsorption–desorption isotherm and SEM images. Thereafter, HJ-M05 was evaluated for the adsorptive removal of phenol from aqueous solution, and Amberlite XAD-4 and XAD-7 were employed as references.

The equilibrium capacities on HJ-M05, XAD-4 and XAD-7 were measured to be 92.43, 46.04 and 36.49 mg/g at an equilibrium concentration of 200 mg/L and the temperature of 308 K. The isosteric adsorption enthalpies on HJ-M05 decreased more greatly than those on XAD-4 and XAD-7 with increasing of the fractional loading, implying a greater degree of the surface energetic heterogeneity of HJ-M05. Both of pseudo-first-order and pseudo-second-order rate equations were suitable for the phenol adsorption on XAD-4 and XAD-7 while the adsorption on HJ-M05 could only be fitted by the pseudo-second-order rate equation. Thomas and Yoon models were shown to be more suitable for fitting the dynamic data than the Clark model and the dynamic capacities for HJ-M05, HJ-55, XAD-4 and XAD-7 were calculated to be 201.7, 178.1, 107.5 and 74.80 mg/g dry resin, respectively, which showed a deviation about 10% the extrapolated values from the Freundlich models. 1% of sodium hydroxide was could completely regenerate the HJ-M05 resin column and the dynamic desorbed amount was 714.1 mg, very close to the dynamic adsorption amount (708.1 mg).

Acknowledgments

The National Natural Science Foundation of China (No. 21174163) and the Shenghua Yuying Project of Central South University are gratefully acknowledged.

Appendix A. Supplementary material

Supplementary data associated with this article can be found, in the online version, at http://dx.doi.org/10.1016/j.cej.2012.04.098.

References

[1] J. Przepiorski, Enhanced adsorption of phenol from water by ammonia-treated activated carbon, J. Hazard. Mater. 135 (2006) 453–456.
[2] A. Rathinam, J.R. Rao, B.U. Nair, Adsorption of phenol onto activated carbon from seaweed: determination of the optimal experimental parameters using factorial design, J. Taiwan Inst. Chem. Eng. 42 (2011) 952–956.
[3] S. Rengaraj, S.H. Moon, R. Sivabalan, B. Arabindoo, V. Murugesan, Removal of phenol from aqueous solution and resin manufacturing industry wastewater using an agricultural waste: rubber seed coat, J. Hazard. Mater. 89 (2002) 185–196.
[4] L.J. Kennedy, J.J. Vijaya, K. Kayalvizhi, G. Sekaran, Adsorption of phenol from aqueous solutions using mesoporous carbon prepared by two-stage process, Chem. Eng. J. 132 (2007) 279–287.
[5] R. Aravindhan, J.R. Rao, B.U. Nair, Application of a chemically modified green macro alga as a biosorbent for phenol removal, J. Environ. Manage. 90 (2009) 1877–1883.
[6] X.W. Zeng, Y.G. Fan, G.L. Wu, C.H. Wang, R.F. Shi, Enhanced adsorption of phenol from water by a novel polar post-crosslinked polymeric adsorbent, J. Hazard. Mater. 169 (2009) 1022–1028.
[7] M.W. Jung, K.H. Ahn, Y.H. Lee, K.P. Kim, I.R. Paeng, J.S. Rhee, J.T. Park, K.J. Paeng, Evaluation on the adsorption capabilities of new chemically modified polymeric adsorbents with protoporphyrin IX, J. Chromatogr. A 917 (2001) 87–93.
[8] G. Kyriakopoulos, D. Doulia, E. Anagnostopoulos, Adsorption of pesticides on porous polymeric adsorbents, Chem. Eng. J. 60 (2005) 1177–1186.
[9] D.S. Grzegorczyk, G. Carta, Adsorption of amino acids on porous polymeric adsorbents-I. Equilibrium, Chem. Eng. Sci. 51 (1996) 807–817.
[10] S.H. Lin, R.S. Juang, Adsorption of phenol and its derivatives from water using synthetic resins and low-cost natural adsorbents: a review, J. Environ. Manage. 90 (2009) 1336–1349.
[11] K. Mohanty, D. Das, M.N. Biswas, Preparation and characterization of activated carbons from *Sterculia alata* nutshell by chemical activation with zinc chloride to remove phenol from wastewater, Adsorption 12 (2006) 119–124.
[12] M. Carmona, A.D. Lucas, J.L. Valverde, B. Velasco, J.F. Rodríguez, Combined adsorption and ion exchange equilibrium of phenol on Amberlite IRA-420, Chem. Eng. J. 117 (2006) 155–160.
[13] I. Dobrevsky, A. Zvezdov, An application of mercury intrusion to explain some peculiarities in the behaviour of the polymeric adsorbent Amberlite XAD-4 during the process of adsorption of phenol from aqueous solutions, Powder Technol. 29 (1981) 205–208.
[14] A.M. Li, Q.X. Zhang, J.L. Chen, Z.H. Fei, C. Long, W.X. Li, Adsorption of phenolic compounds on Amberlite XAD-4 and its acetylated derivative MX-4, React. Funct. Polym. 49 (2001) 225–233.
[15] L.E. Vera-Avila, J.L. Gallegos-Perez, E. Camacho-Frias, Frontal analysis of aqueous phenol solutions in amberlite XAD-4 columns: implications on the operation and design of solid phase extraction systems, Talanta 50 (1999) 509–526.
[16] M.S. Bilgili, Adsorption of 4-chlorophenol from aqueous solutions by xad-4 resin: isotherm, kinetic, and thermodynamic analysis, J. Hazard. Mater. 137 (2006) 157–164.
[17] J.H. Huang, X.G. Wang, K.L. Huang, Adsorption of p-nitroaniline by phenolic hydroxyl groups modified hyper-cross-linked polymeric adsorbent and XAD-4: a comparative study, Chem. Eng. J. 155 (2009) 722–727.
[18] P.A.M. Freitas, K. Iha, M.C.F.C. Felinto, M.E.V. Suárez-Iha, Adsorption of di-2-pyridyl ketone salicyloylhydrazone on Amberlite XAD-2 and XAD-7 resins: characteristics and isotherms, J. Colloid Interface Sci. 323 (2008) 1–5.
[19] R. Navarro, I. Saucedo, C. Gonzalez, E. Guibal, Amberlite XAD-7 impregnated with Cyphos IL-101 (tetraalkylphosphonium ionic liquid) for Pd(II) recovery from HCl solutions, Chem. Eng. J. 185 (186) (2012) 226–235.
[20] A. Hosseini-Bandegharaei, M.S. Hosseini, M. Sarw-Ghadi, S. Zowghi, E. Hosseini, H. Hosseini-Bandegharaei, Kinetics, equilibrium and thermodynamic study of Cr(VI) sorption into toluidine blue o-impregnated XAD-7 resin beads and its application for the treatment of wastewaters containing Cr(VI), Chem. Eng. J. 160 (2010) 190–198.
[21] N. Fontanals, P.A.G. Cormack, D.C. Sherrington, Hypercrosslinked polymer microspheres with weak anion-exchange character: preparation of the microspheres and their applications in pH-tuneable, selective extractions of analytes from complex environmental samples, J. Chromatogr. A 1215 (2008) 21–29.
[22] N. Fontanals, P.A.G. Cormack, D.C. Sherrington, R.M. Marcé, F. Borrull, Weak anion-exchange hypercrosslinked sorbent in on-line solid-phase extraction–liquid chromatography coupling to achieve automated determination with an effective clean-up, J. Chromatogr. A 1217 (2010) 2855–2861.
[23] M.P. Tsyurupa, V.A. Davankov, Porous structure of hypercrosslinked polystyrene: state-of-the-art mini-review, React. Funct. Polym. 66 (2006) 768–779.
[24] C.L. He, K.L. Huang, J.H. Huang, Surface modification on a hyper-cross-linked polymeric adsorbent by multiple phenolic hydroxyl groups to be used as a specific adsorbent for adsorptive removal of p-nitroaniline from aqueous solution, J. Colloid Interface Sci. 342 (2010) 462–466.
[25] J.H. Huang, Adsorption properties of a microporous and mesoporous hyper-crosslinked polymeric adsorbent functionalized with phenoxy groups for phenol in aqueous solution, J. Colloid Interface Sci. 39 (2009) 296–301.
[26] A. Li, Q. Zhang, H. Wu, Z. Zhai, F. Liu, Z. Fei, C. Long, Z. Zhu, J. Chen, A new amine-modified hypercrosslinked polymeric adsorbent for removing phenolic compounds from aqueous solutions, Adsorp. Sci. Technol. 22 (2004) 807–820.
[27] V.C. Srivastava, B. Prasad, I.M. Mishra, I.D. Mall, M.M. Swamy, Prediction of breakthrough curves for sorptive removal of phenol by bagasse, fly ash packed bed, Ind. Eng. Chem. Res. 47 (2008) 1603–1613.
[28] B.H. Hameed, A.A. Ahmad, N. Aziz, Isotherms, kinetics and thermodynamics of acid dye adsorption on activated palm ash, Chem. Eng. J. 133 (2007) 195–203.
[29] A.B. Albadarin, C. Mangwandi, A.H. Al-Muhtaseb, G.M. Walker, S.J. Allen, M.N.M. Ahmad, Kinetic and thermodynamics of chromium ions adsorption onto low-cost dolomite adsorbent, Chem. Eng. J. 179 (2012) 193–202.
[30] C.P. Wu, C.H. Zhou, F.X. Li, Experiments of Polymeric Chemistry, Anhui Science and Technology Press, Hefei, 1987.
[31] B.L. He, W.Q. Huang, Ion Exchange and Adsorption Resin, Shanghai Science and Technology Education Press, Shanghai, 1995.
[32] J.H. Ahn, J.E. Jang, C.G. Oh, S.K. Ihm, J. Cortez, D.C. Sherrington, Rapid generation and control of microporosity, bimodal pore size distribution, and surface area in Davankov-type hyper-cross-linked resins, Macromolecules 39 (2006) 627–632.
[33] C.L. He, J.H. Huang, C. Yan, J.B. Liu, Li.B. Deng, K.L. Huang, Adsorption behaviors of a novel carbonyl and hydroxyl groups modified hyper-cross-linked poly(styrene-co-divinylbenzene) resin for β-naphthol from aqueous solution, J. Hazard. Mater. 180 (2010) 634–639.
[34] D.M. Ruthven, Principles and Adsorption and Adsorption Processes, Willey, New York, 1984.

[35] D.D. Duong, Adsorption Analysis: Equilibria and Kinetics, World Scientific Publishing, Singapore, 1998.
[36] I. Langmuir, The constitution and fundamental properties of solids and liquids. Part I. Solids, J. Am. Chem. Soc. 38 (1916) 2221–2295.
[37] H.M.F. Freundlich, Über die adsorption in lösungen, Z. Phys. Chem. 57A (1906) 385–470.
[38] R. Sips, On the structure of a catalyst surface, J. Chem. Phys. 16 (1948) 490–495.
[39] H.T. Li, M.C. Xu, Z.Q. Shi, B.L. He, Isotherm analysis of phenol adsorption on polymeric adsorbents from nonaqueous solution, J. Colloid Interface Sci. 271 (2004) 47–54.
[40] J.H. Huang, K.L. Huang, S.Q. Liu, Q. Luo, M.C. Xu, Adsorption properties of tea polyphenols onto three polymeric adsorbents, with amide group, J. Colloid Interface Sci. 315 (2007) 407–414.
[41] D.D. Do, H.D. Do, A new adsorption isotherm for heterogeneous adsorbent based on the isosteric heat as a function of loading, Chem. Eng. Sci. 52 (1997) 297–310.
[42] B.J. Pan, B.C. Pan, W.M. Zhang, Q.R. Zhang, Q.X. Zhang, S.R. Zheng, Adsorptive removal of phenol from aqueous phase by using a porous acrylic ester polymer, J. Hazard. Mater. 57 (2008) 293–299.
[43] S. Lagergren, About the theory of so-called adsorption of soluble substances, Kungliga Svenska Vetenskapsakademiens, Handlingar, Band 24 (1898) 1–39.
[44] Y.S. Ho, Review of second-order models for adsorption systems, J. Hazard. Mater. 136 (1998) 681–689.
[45] D.M. Ruthven, S. Farooq, K.S. Knaebel, Pressure Swing Adsorption, VCH, New York, 1994.
[46] H.C. Thomas, Heterogeneous ion exchange in a flowing system, J. Am. Chem. Soc. 66 (1944) 1664–1666.
[47] R.M. Clark, Evaluating the cost and performance of field-scale granular activated carbon systems, Environ. Sci. Technol. 21 (1987) 573–580.
[48] Y.H. Yoon, J.H. Nelson, Application of gas adsorption kinetics. I. A theoretical model for respirator cartridge service time, Am. Indian Hygiene Assoc. J. 45 (1984) 509–516.